RESPONSE OF OFFSHORE STRUCTURES UNDER THE EFFECT OF REAL SEA STATES INCLUDING STRUCTURAL AND SOIL NONLINEARITIES

Konstantinos Chatziioannou, Vanessa Katsardi, Apostolos Koukouselis and Euripidis Mistakidis

Laboratory of Structural Analysis and Design, Department of Civil Engineering,
University of Thessaly, Volos, GR-38334, Greece
e-mail: emistaki@uth.gr ; web page: http: http://lsad.civ.uth.gr/

Keywords: Fluid-structure interactions**,** fully nonlinear waves**,** geometrically nonlinear analysis

Abstract. *This work highlights the importance of the consideration of nonlinearities in the analysis and design of deep water platforms; referring both to the calculation of the wave loading and to the structural analysis. More specifically, the wave loading is based on a fully nonlinear three-dimensional wave model capable of accurately representing a realistic distribution of wave energy in both the frequency and the directional domains (Bateman, Swan & Taylor 2001, 2003). For reference, commonly applied design wave solutions are also considered. On the other hand, in the field of structural analysis, three cases are considered for comparison, linear, linear analysis for the structural members with nonlinear soil-structure interaction and geometrically nonlinear analysis with nonlinear soil-structure interaction. The structural calculations are performed using the structural analysis software SAP2000, however, a special programming interface was developed in order to calculate the wave loading and to directly apply the generated loads on the structural members. The example treated in the context of the present paper is a compliant tower set-up in deep water. The results show that the consideration of the nonlinear particle kinematics in the wave loading and the consideration of the geometrically nonlinear structural response leads to significant differences with respect to the common design methods in both the displacements and stresses of the structure.*

1 INTRODUCTION

The purpose of this paper is to examine the response of an offshore structure located in deep water under the effect of wave and wind loads. In terms of wave calculations, the paper provides fully nonlinear or exact calculations of predetermined design wave conditions relevant to the assessment of the loads acting on a compliant tower, grounded in a large water depth, and also provides comparisons between these results and predictions based upon the commonly applied design wave solutions. In terms of the response of the structure, the linear and geometrically nonlinear responses are calculated, based on static analysis. More specifically, the structure that is examined is a compliant tower (Fig.1), located in deep water in the area between Singapore and Kuala Lumpur. The tower has an overall height of 534m, the 510m of which are located beneath the water level and the rest 24m include the decks above the surface. The foundation of the structure consists of three piles.

With the key goal being an assessment of the accuracy of the commonly applied design wave models, a fully nonlinear three dimensions wave model proposed by Bateman, Swan, & Taylor (2001) and Bateman, Swan, & Taylor (2003) [1-2] (BST) was used. The results of the BST are directly compared with those of the commonly applied design wave models: (a) Directional (3D) Linear Random Wave Theory (LRWT), (b) Directional (3D) Second-order random wave theory [3] (SD) and (c) Stokes fifth-order steady wave theory [4].

Applying the wave forces yielded by the above theories, the base shear and total overturning moments associated with the compliant tower are calculated. Moreover, the corresponding peak displacement and rotation angles are determined using (a) linear analysis for the structural members and the soil (L-LS), (b) linear analysis for the structural members with nonlinear soil-structure interaction(L-NLS) and (c) geometrically nonlinear analysis with nonlinear soil-structure interaction (GN-NLS). In order to complete these analyses, a well-known finite element software for static and dynamic analysis of structures was used (SAP2000). Moreover, a special programming interface was developed in order to calculate and directly apply the wave loads on the structural members.

Bottom fixed and flexible offshore platforms should be designed based on dynamic analysis of the wave loads. Indeed, a static analysis describes only part of the problem since it ignores the dynamic response and the possibility of resonance phenomena of the structure when the natural frequency of the structure is hit. The latter may occur either when the structure is subject to *smaller* waves than the design wave and their frequency is close to the natural frequency of the wave, or when the structure is subject to nonlinear waves and higher order

components are close to the natural frequency of the waves [5]. For this reason, the dynamic analysis of such structures includes nonlinear steady waves that most times interact with idealized structures [6]. However, a more realistic representation of the sea-state, including unsteadiness and nonlinearity was investigated in [7] and included the static effect of linear and weakly nonlinear random waves to the response of an idealized jacket-type structure. Later, [8] performed dynamic analysis of an idealized jack-up structure, representing the largest wave with the linear *NewWave* theory [9] (for more details refer to Section 3).The novelty of the present research is that it investigates the effect of an exact representation of the sea state, incorporating all on a non-idealized compliant tower consisting of more than 2000 elements. The authors recognize the necessity of performing a dynamic analysis, however, the early finding of this research are presented in this paper, where linear and large displacement theory static analyses, as well as a nonlinear representation of the soil-structure interaction have been employed.

2 STRUCTURE - SOIL MODELING

The structure was simulated with 1960 frame elements and 25 area elements in the upper deck. The base material is steel A36 and in some cases C50/60 grout is used to fill the tubular structural members. The compliant tower consists of 19 typical bays (Figure 2) and the frame sections of the members vary with depth.

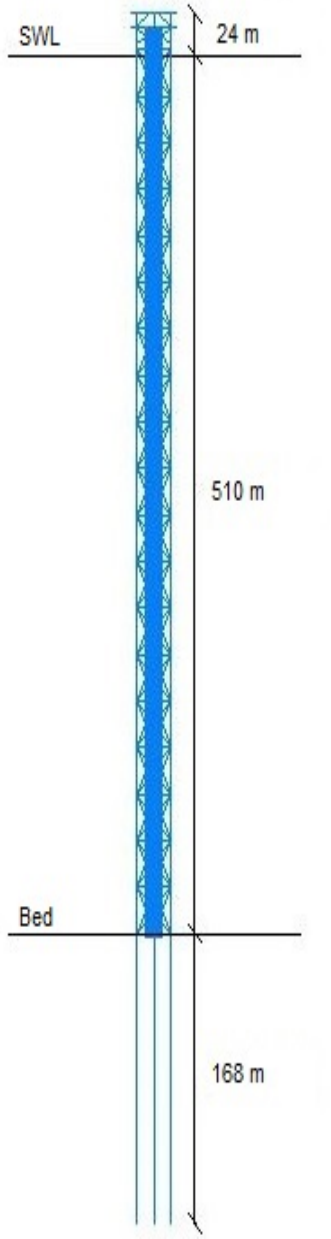

Figure 1. Typical elevation of the structure.

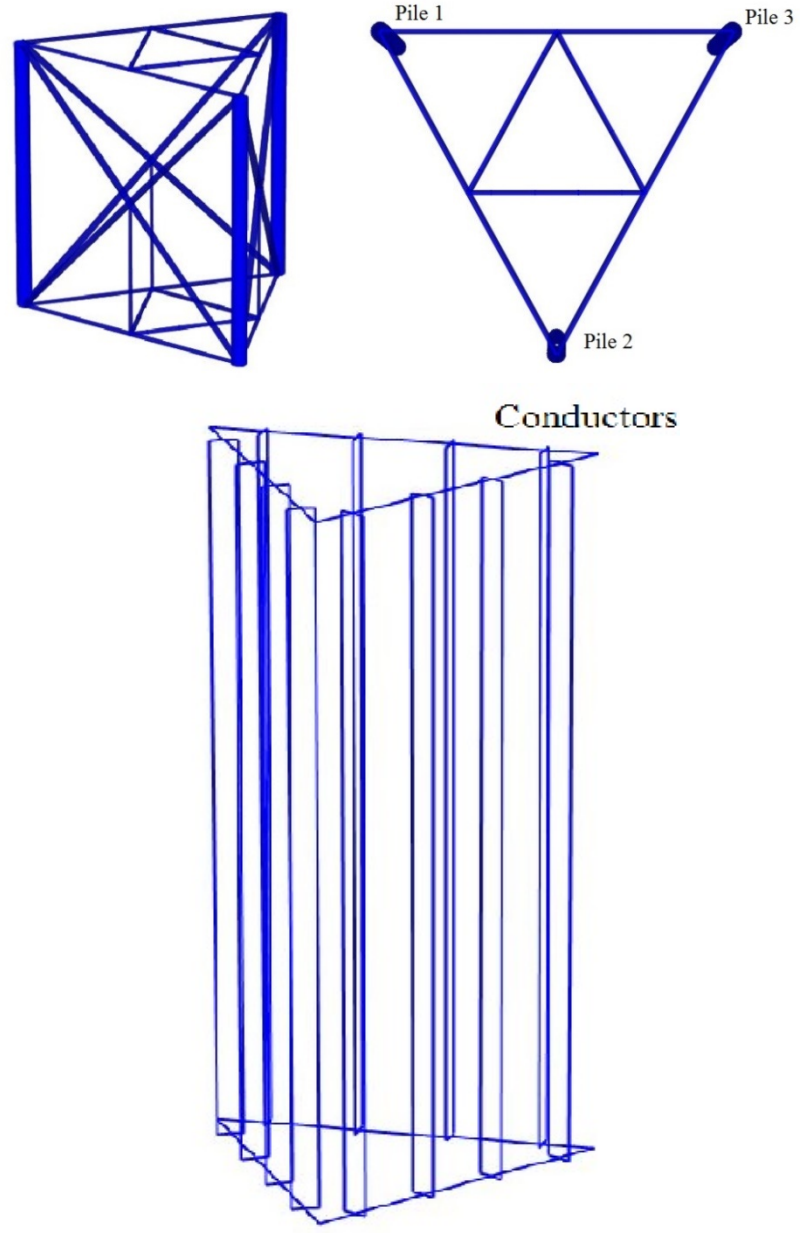

Figure 2. Typical bay and conductors.

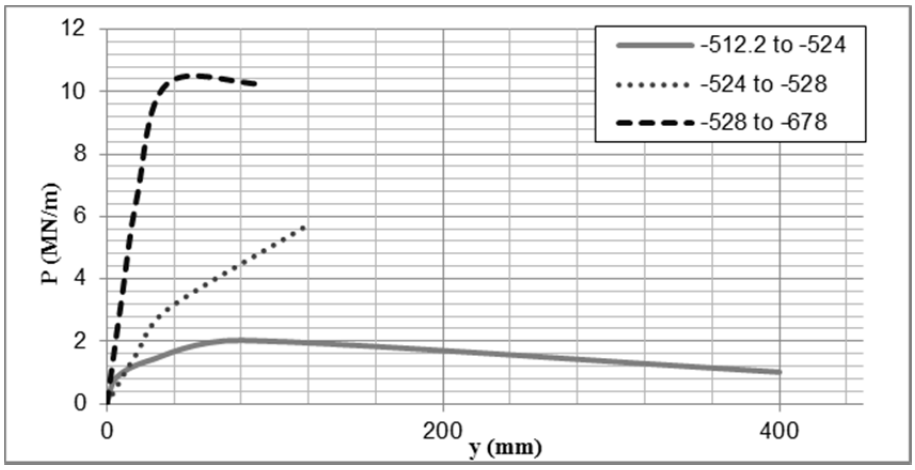

(a)

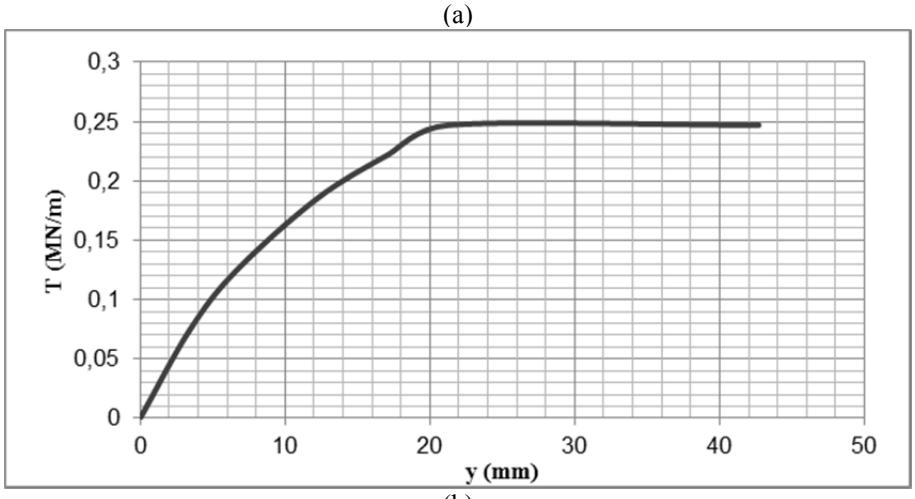

(b)

Figure 3. Soil response curves for the (a) horizontal and (b) vertical direction.

Each typical bay is connected with the above with 24 conductors. These are the frame elements that are depicted in Figure 2 and they are placed in the inner triangle of the typical bay. The diameters of their frame sections vary from 0.4m to 0.6m. The foundation of the structure consists of three piles with a length of 168m extending from -510m to -678 m. The soil-structure interaction was modelled with nonlinear springs. Figure 3(a) shows the soil resistance in the lateral direction. The upper soil layers provide low resistance in the horizontal displacements while the resistance increases with depth. Furthermore, in Figure 3(b) the vertical resistance of the soil is also depicted.

3 ENVIROMENTAL CONDITIONS

Within the present calculations, the fully nonlinear wave models are used in conjunction with the linear *NewWave* theory [9]; the later providing a linear representation of the most probable shape of a large wave of given crest elevation or wave height. In simple terms, the *NewWave* model represents a given sea state in terms of a large number of frequency components having both random phase and random amplitude, and shows that the most probable shape of a large wave arises when the relative phasing reduces to zero and the amplitudes of the components are proportional to the underlying frequency spectrum, $S_{\eta\eta}(\omega)$. In the present study the wave conditions considered were specified *a priori*; identified as the key wave cases observed in the area by the designers of the structure. Before outlining the work undertaken and the results achieved, it is important to consider the nature of the extreme wave event under consideration; full details of which are given in Table 1. With a water depth of d=510m and a spectral peak period of $T_p = 14.53$s, the effective water depth $k_p d$, where k_p is the wave number corresponding to the spectral peak, corresponds to $k_p d$=9.7≫3; characterizing the wave conditions as being in deep water. In the unsteady or irregular wave simulations (involving the fully nonlinear wave model, the linear random wave theory and the second-order random wave theory) the wave events arise

within a sea state which is modelled using a JONSWAP [10] spectrum with a peak enhancement factor of γ=3.3. In the steady or regular wave simulations (involving the 5th-order), the solutions were matched to the maximum wave height (H_{max}) and the associated trough-to-trough wave period (T_{trtr}). The calculations were undertaken assuming the sea state was directionally spread; characterised as having a Mitsuyasu [11], or cos^{2s}, spreading parameter of $s = 7$. These values are applied uniformly to all frequency components, with $s = 7$ representing a short-crested sea state, corresponding to a wrapped normal distribution with a standard deviation of approximately $\sigma_\theta = 30^o$.

In the case of applying a LRWT and in order to encounter the well-known effects of high-frequency contamination regarding the kinematics calculations, leading to the gross over-prediction of the largest near-surface velocities, an empirical correction or stretching [12] is applied. Furthermore, in the case of applying the steady wave solutions, the effectiveness of a simple Velocity Reduction Factor, Φ, to account for the directional spread is also considered. For the specified sea state the appropriate reduction factor is calculated as $\Phi = 0.88$. More details on the application of the wave theories and wave models and the numerical results are given in the relevant publication of the author's team [13].

In Table 1, two wave heights are noted. The significant wave height $H_s = 6.077$m and the maximum wave height calculated as $H_{max} = 1.85H_S \simeq 11.21$m, based on the DNV 2000 Classification Notes [14], corresponding to the specific wave conditions associated with the design storm. Although it is well understood that these two wave heights are part of the same storm and should not be investigated separately, for the sake of investigating the effect of wave steepness they will be considered as two separate maximum wave heights, as if they were part of two independent wave conditions.

Water depth	$d = 510$m
Spectral Shape, $S\eta\eta$ (ω)	JONSWAP
Peak enhancement factor	$\gamma = 3.3$
Spectral peak period	$T_p = 14.53$s
Significant wave height	$H_s = 6.077$m
Maximum wave height ($H_{max} \simeq 1.85H_s$)	$H_{max} = 11.21$m
Associated wave period	$T_{trtr} = 12.5$s
Velocity reduction factor	$\Phi = 0.88$
Wind speed	$V_z = 65.1$m/s

Table 1: Specified wave conditions.

4 CALCULATION OF THE FORCES ON STRUCTURAL MEMBERS

In order to calculate the forces on the structural elements, the well-known Morison's equation was used,

$$F_{xi} = C_D \frac{1}{2}\rho D_i \int u^2 dz + C_M \frac{\pi {D_i}^2}{4} \int \frac{\partial u}{\partial t} dz \quad (1)$$

where ρ is the water density, D_i the diameter of element i and C_D and C_M the drag and inertia coefficients respectively. Values for the latter were taken from the API 1993 [15] for smooth cylinders with small diameter, as C_D = 0.65 and C_M = 1.60 respectively. Due to the size and complexity of the structure, it was necessary to develop appropriate software in order to automate the load application process. The programming interface was built on the Visual Basic platform. The code that was generated takes as input the wave height, the wave period, the depth, the wave angle in the horizontal plane, the existence of current, the planar coordinates of the wave crest (x, y) and the C_M, C_D constants and calculates the wave number (k) by solving the dispersion relation. In the case of Airy or Stokes 2nd, the dispersion equation has the following expression.

$$\frac{\omega}{k} = \sqrt{\frac{gtanh(kd)}{k}} + Current\ Velocity \quad (2)$$

In the case of Stokes 5th the dispersion equation is nonlinear and according to Fenton [4] is transformed as follows:

$$\omega^2 = gktanh(kd)(1 + \varepsilon^2 C_1 + \varepsilon^4 C_2) \quad (3)$$

where:

$$C_1 = \frac{8\cosh(kd)^4 - 8\cosh(kd)^2 + 9}{8\sinh(kd)^4}$$

$$C_2 = (3840\cosh(kd)^{12} - 4096\cosh(kd)^{10} - 2592\cosh(kd)^8 - 1008\cosh(kd)^6 + 5944\cosh(kd)^4 - 1830\cosh(kd)^2 + 147)/(512\sinh(kd)^{10}(6\cosh(\mathrm{kd})^2 - 1))$$

$$\varepsilon = kH/2$$

The developed code allows the user to select the appropriate wave theory or model (Airy, Stokes 2nd, Stokes 5th, LRWT, SD and BST,) and according to the wave properties, the frames sections, the depth of the frame's edges and their coordinates, it generates a static load by applying Morison's equation. When the unsteady wave solutions are applied, the kinematics are calculated in separate codes and are then used as an input to the new code in order to calculate forces according to Eqn. (1).

Moreover, the dead load and the buoyancy forces on the members are also calculated using the developed software by retrieving the length, the cross area as well as the weight of the material, and generates the dead load of each element applying them as point forces on the two edge nodes of each member. The code is also programed to work with grouted sections. In a similar way, in case the member is flooded, the volume (V) of the members is calculated and according to the length of the member the buoyancy forces are generated.

Furthermore, this special programming interface consists of a third part which is responsible for the simulation of the soil. This part of the code retrieves the information of the P-Y, T-Z curves from a spreadsheet, processes the data, takes as input the starting depth of the foundation and generates the appropriate spring properties of the support nodes depending on their depth.

Finally, the wind load was generated according to API 4F-2008 [16]

5 WAVE STRUCTURE INTERACTION

In Table 3 the total displacement of the top of the tower and the total rotation angle for the geometrically nonlinear analysis are presented. Comparing the cases without the wind impact it is observed that, irrespective of the wave theory used to describe the wave loading, the increase in the peak displacement and rotation angle is much larger than the wave height increase; i.e. H_{max} is only 84% larger than H_s, while the corresponding peak displacement and rotation angle is more than 300% larger, using the steady wave description (Stokes 5th), and more than 165% larger, using the unsteady wave description (BST). This is to be expected since the forces are proportional to u^2 (Eqn. (1)), hence the increase in forces is not linearly dependent upon the increase in wave heights. Introducing the effect of the wind, it is easily observed that it dominates the phenomenon for both wave cases and this is because the wind speed is very large making the changes in the results due to the different wave theories much less severe. Furthermore, as for the validity of the wave theories, for all the scenarios investigated, the steady wave solution under-predicts both the peak displacement and the rotation angle as up to 112% for the cases without the wind impact, and up to 12% for the cases with the wind impact, compared with the fully nonlinear solution. Furthermore, although it has been shown by earlier investigation of the authors [13] that the unsteady linear or weakly nonlinear solutions describe much better the surface elevations and the underlying kinematics (LRWT and SD), they over-predict the peak displacement and the rotation angle as up to 14% for the cases without the wind impact, and up to 5.6% for the cases with the wind impact, compared with the fully nonlinear solution. With the peak-displacement and the rotation angle being of critical importance for the safety and function of the working staff, the structure and the machinery of the tower, these discrepancies should be taken very seriously into account.

Conditions		Stokes 5th	LRWT	BST
H_s	Δx (m)	0.81	1.92	1.72
	θ (deg)	0.15	0.30	0.27
$H_s + W$	Δx (m)	15.12	17.04	16.70
	θ (deg)	2.12	2.35	2.31
H_{max}	Δx (m)	3.28	5.32	4.58
	θ (deg)	0.49	0.76	0.66
$H_{max} + W$	Δx (m)	18.46	21.91	20.68
	θ (deg)	2.54	2.95	2.80

Table 2: Top Displacement, Δx, and Rotation Angle, θ, with and without the effect of the wind W (V_z= 65.1m/s), using Large Displacement Theory for H_s=6.077m and H_{max} = 11.21m.

In Tables 3, 4 and 5 comparisons of the calculations of the base shear and the total overturning moment are presented. The former were calculated using linear analysis for the structural members and the latter using geometrically nonlinear theory. In the last two cases the nonlinearity of the soil has been taken into account. The compliant tower, as described before, depending on the scenario, was subject to wave loading or wave and wind loading. The waves were described by either a nonlinear steady wave solution (Stokes 5th) or by two unsteady

wave solutions; LRWT (the kinematics empirically stretched) and BST for the smaller wave height (H_s) and SD and BST for the largest wave case (H_{max}).

Regarding the base shear, the differences in the results, based on all scenarios applying linear or geometrically nonlinear analysis, are negligible. On the other hand, for all the considered scenarios, using geometrically nonlinear analysis, the overturning moment is increased. This is actually a consequence of the fact that the horizontal displacements are significantly larger in the case of the geometrically nonlinear analysis and, therefore, the moment-arm of the structure's gravity force is also significantly larger compared to the case of the linear analysis.

Regarding the validity of the wave theories or solutions applied, as noted in the results concerning the top displacement and the rotation angle outlined in Table 2 for all the scenarios investigated, applying the steady wave solution leads to an under-prediction for both the base shear and the total overturning moment. Indeed, applying the Stokes 5th solution, the base shear is smaller than the one predicted when applying the BST by more than 54% for the H_s = 6.077m case and more than 29% for the H_{max} = 11.21m case (without the wind impact). The corresponding values for both cases with the wind impact, are 8.2% and 9.4% respectively (Table 3). The overturning moment is calculated smaller when applying the Stokes 5th solution than when applying the BST by more than 51% for the H_s = 6.077m case, by almost 30% for the H_{max} = 11.21m case (without the wind impact), and by at least 7.2% for the cases with the wind impact. Furthermore, again, despite that the unsteady linear or weakly nonlinear solutions describe much better the surface elevations (LRWT and SD) and the underlying kinematics (LRWT and SD) as shown in [11], the adoption of these solutions in loading calculations leads to an over-prediction of both the base shear and the total overturning moment compared to the application of the exact solution (BST) by as much as 10% for the cases without the wind impact and by as much as 4% for the cases with the wind impact (Tables 4 and 5). These significant differences are very important as they may either lead to design-failure (if a steady solution is to be applied) or to an uneconomical design (if a LRWT or SD solution is to be applied).

	H_s			H_s+W	
Stokes 5th	BST	LRWT	Stokes 5th	BST	LRWT
242	527	584	3194	3479	3536
	+54.2%	+58.6%		+8.2%	+9.7%
	H_{max}			$H_{max}+W$	
Stokes 5th	BST	SD	Stokes 5th	BST	SD
936	1326	1516	3749	4319	4328
	+29.4%	+38.2%		+9.4%	+13.4%

Table 3: Comparisons of the base shear (in kN) arising due to H_s and H_{max} with and without the wind.

	H_s			H_s+W	
Stokes 5th	BST	LRWT	Stokes 5th	BST	LRWT
123.2	254.6	282.1	1682	1813.5	1841
	+51.6%	+56.3%		+7.2%	+8.6%
	H_{max}			$H_{max}+W$	
Stokes 5th	BST	SD	Stokes 5th	BST	SD
468.7	641.1	734.9	1955.6	2128.4	2222.1
	+26.9%	+36.2%		+8.1%	+12%

Table 4: Comparisons of the overturning moment (in MNm) arising due to H_s and H_{max}, with and without the wind, using linear analysis**.**

	H_s			H_s+W	
Stokes 5th	BST	LRWT	Stokes 5th	BST	LRWT
127.1	262.8	291.3	1754.7	1893.4	1922.5
	+51.6%	+56.4%		+7.3%	+8.7%
	H_{max}			$H_{max}+W$	
Stokes 5th	BST	SD	Stokes 5th	BST	SD
484.2	662.3	759.9	2043.5	2225.8	2325.3
	+26.9%	+36.3%		+8.2%	+12.1%

Table 5: Comparisons of the overturning moment (in MNm) arising due to H_s and H_{max}, with and without the wind, using geometrically nonlinear analysis.

6 SOIL STRUCTURE INTERACTION

This part of the paper examines the interaction between the soil and the structure. In order to focus on the interaction between these two and for brevity, the results that are presented are derived from the BST wave model only. When necessary, the differences between linear, nonlinear soil-structure and geometrically nonlinear analysis are compared. In linear analysis, the first part of the P-Y, T-Z curves is used as effective stifness and therefore, stresses from the upper structure are absorbed in the upper soil layers. On the other hand, in geometrically nonlinear analysis, the distribution of the stresses is different due to the fact that the soil enters the plastic domain of the stress–strain diagram. Taking into consideration the geometry of the foundation, it is obvious that as the wave propagates towards the structure, the structure has the tendency to rotate around the vertical axis that coincides with the geometrical center of the three piles.

Figure 4 shows that Pile 1 has the largest horizontal deflections for all the analysis cases and is the only one of the three piles that tends to be extruded from the soil. The differences between linear and geometrically nonlinear analyses are obvious for both directions, not only in terms of the maximum displacements but also in the deformed shape of the pile. The differences that arise when the nonlinearities are being taken into consideration are obvious. In both nonlinear (L-NLS) and geometrically nonlinear (GN-NLS) analyses the kinematic results are about twise as large in comparison with those yielded by the linear analysis (L-LS). Furthermore, between nonlinear (L-NLS) and geometrically nonlinear (GN-NLS) analysis it can be derived that both in the lateral and vertical directions, the effect of the structure's weight increases the displacements by at 6%. From Figure 5 it can be observed that Pile 2 has a deformed shape similar to that of Pile 1 in the horizontal direction. However, things are different in the vertical direction. This is due to its tendecy to overturn around the geometrical center.

Pile 3 maintains the same deformed shape in the horizontal direction as the other two; however, in the vertical direction this pile is under compression. Once more, the differences betweeen linear and geometrically nonlinear analyses are enormous. On the orther hand, the deformed shape in nonlinear (L-NLS) and geometrically nonlinear analyses (GN-NLS) are similar especially in the horizontal direction.

Figures 7, 8 and 9 show the response of the soil under each of the piles for the nonlinear soil-structure interaction (L-NLS) and geometrically nonlinear analysis (GN-NLS). It can be derived that in both cases, in the horizontal direction the soil reaches about 80% of its total strength in the upper layers. In the vertical direction, the soil exhausts almost completely its shear capacity along the pile's length. On the other hand, according to Figure 8, Pile 2 is the one with the minimum deflections. This occurs due to the position of the pile. Furthermore, the soil under Pile 1 and Pile 3 are under larger tensions and compresion in the geometrically nonlinear analysis while the oposite happens in Pile 2.

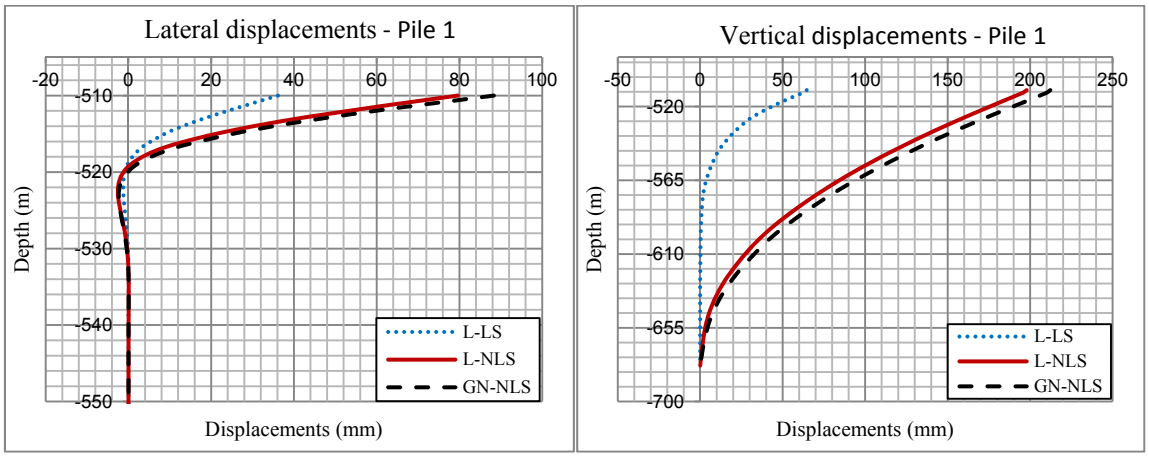

Figure 4: Lateral – Vertical displacements of Pile 1.

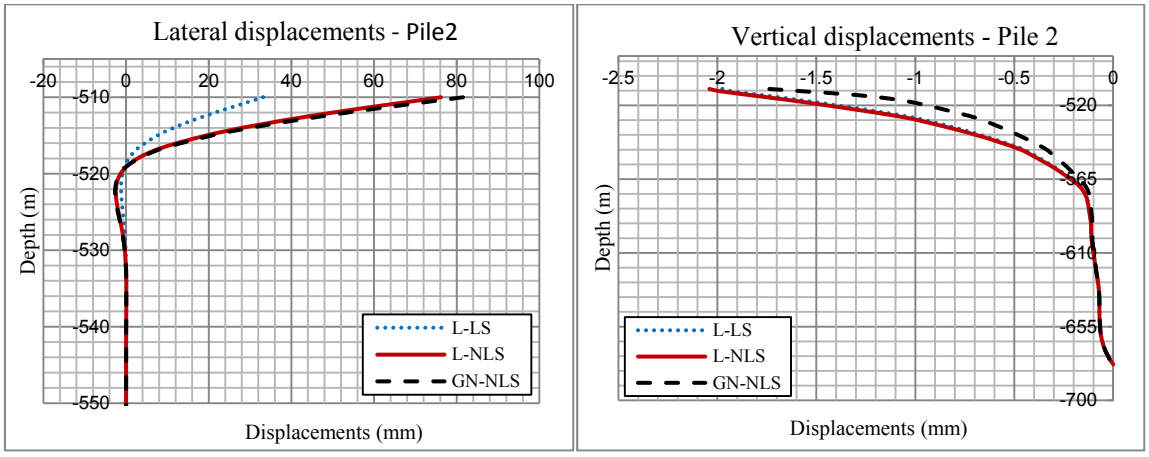

Figure 5: Lateral - Vertical displacements of Pile 2.

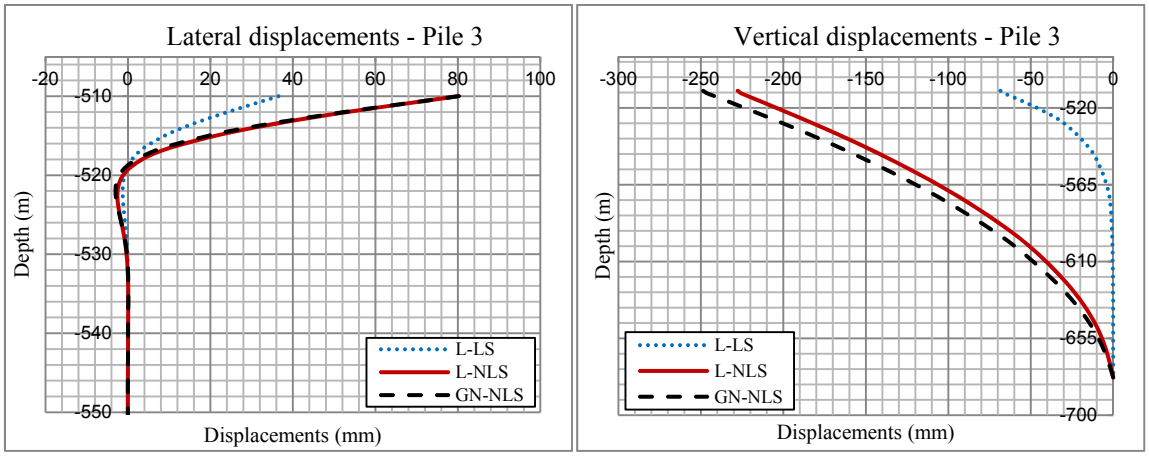

Figure 6: Lateral - Vertical displacements of Pile 3.

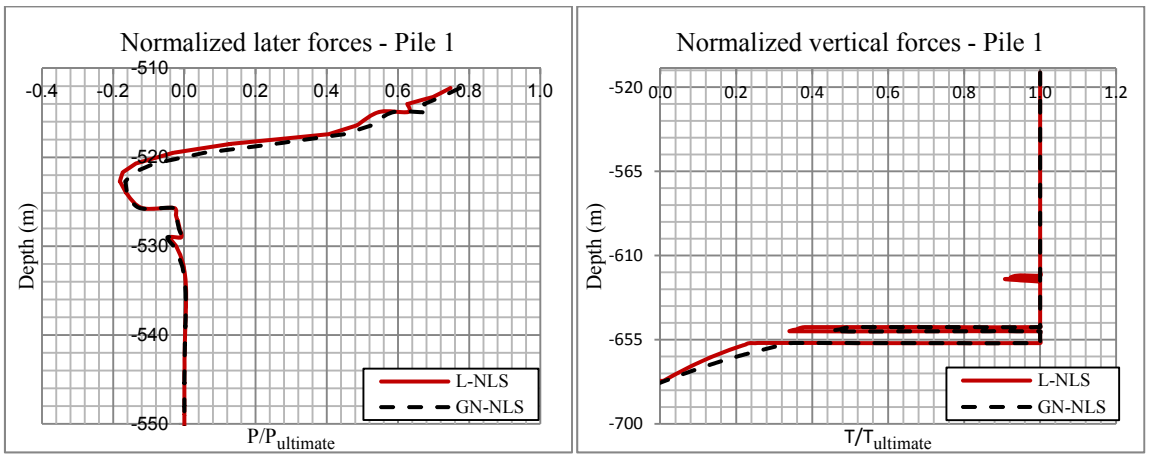

Figure 7: Soil reactions under Pile 1

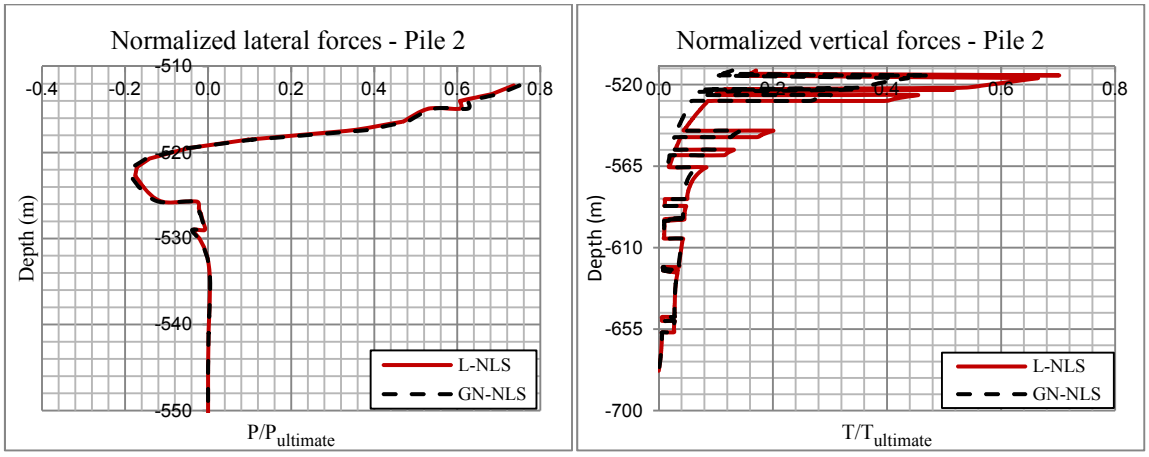

Figure 8: Soil reactions under Pile 2

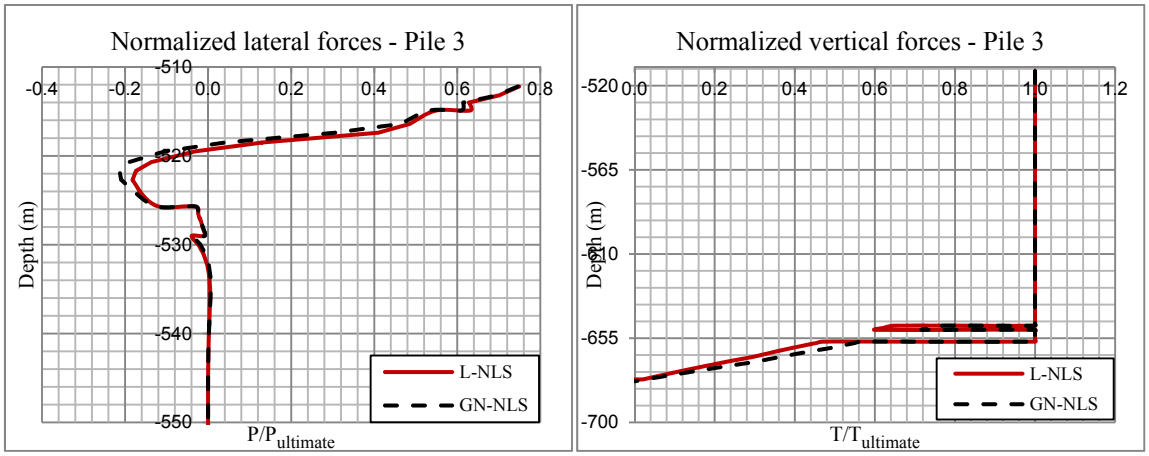

Figure 9: Soil reactions under Pile 3.

7 CONCLUSIONS

This paper highlights the importance of the calculation of the nonlinear extreme wave kinematics appropriate for load calculations of the elements of a platform in deep water. The response of the structure under linear and geometrically nonlinear analysis has been investigated based on numerical calculations undertaken using a fully nonlinear three-dimensional wave model capable of accurately representing a realistic distribution of wave energy in both the frequency and the directional domains (BST). As for the validity of the applied wave solutions it was found that applying a steady wave solution (Stokes 5th), as it is often done in design, leads to very significant (up to 121%) underestimates, compared to the BST, of all the crucial factors of the function and design of the structure; the former referring to the peak-displacement and the rotation angle and the latter to the base shear and total overturning moment and may lead to design-failure. On the other hand, when an unsteady solution is applied (LRWT or SD) then the calculations lead to overestimates of the corresponding factors (up to 14%) leading to an uneconomical design of the structure. Furthermore, the differences between linear (L-LS), nonlinear soil-structure interaction (L-NLS) and fully nonlinear analyses (geometrically nonlinear analysis with nonlinear soil-structure interaction - GN-NLS) are profound. Irrespective of the adopted wave theory, the nonlinear (L-NLS) and geometrically nonlinear (GN-NLS) analyses lead to significant discrepancies. For example, from the nonlinear as well as from the geometrically nonlinear analysis it becomes obvious that the soil reaches about 80% of its total strength under Pile 1 and Pile 3, something that cannot be observed in the case of linear analysis. Finally, the comparisons that concern the displacements of the piles using nonlinear or geometrically nonlinear analysis are significant. Indeed, in both the vertical and horizontal directions, the displacements are almost two times larger than in the case of linear analysis. The above discrepancies are of critical importance for the safety and function of the working staff, the structure and the machinery of the tower.

ACKNOWLEDGEMENTS

The authors would like to thank Prof. Chris Swan from Imperial College, London for the permission to use the numerical code that incorporates the BST model for this research. Moreover, the authors would like to thank Prof. Demos Angelides from Aristotle University of Thessaloniki for his comments for improving this work and his helpful discussions and Dr. Vasilis Mamatsopoulos for providing the structural data for the deep water platform treated in this paper.

REFERENCES

[1] Bateman, W. J. D., C. Swan, & P. H. Taylor (2001). "On the efficient numerical simulation of directionally-spread surface water waves". *Journal of Computational Physics*, Vol 174, pp. 277–305.
[2] Bateman,W. J. D., C. Swan, & P. H. Taylor (2003). "On the calculation of the water prticle kinematics arising in a directionally spread wavefield". *Journal of Computational Physics*, Vol. 186, pp. 70–92.
[3] Sharma, J. N. & R. G. Dean (1981). "Second-order directional seas and associated wave forces". *Society of Petroleum Engineering Journal*, Vol 4, pp. 129–140.
[4] Fenton, J. D. (1985). "A fifth order stokes' theory for steady waves". *J. Waterway, Port, Coastal and Ocean Eng*. Vol. 111, pp. 216–234.
[5] Harleman, D. R. F.,W. C. Nolan, & V. C. Honsinger (1962). "Dynamic analysis of offshore structures". In Proceedings of 8th Conference on Coastal Engineering, Mexico City, Mexico, 1962, pp. 482–499.
[6] Williams, M. S., R. S. Thompson, & G. T. Houlsby (1998). "Nonlinear dynamic analysis of oshore jack-up units". Computers and Structures Vol. 69, pp. 171 – 180.
[7] Kareem, A., C. C. Hsieh, & M. A. Tognarelli (1998). "Frequencydomain analysis of offshore platform in non-gaussian seas". Journal of Engineering Mechanics Vol. 124(6), pp. 668–683.
[8] Cassidy, M., R. Taylor, & G. Houlsby (2001). "Analysis of jackup units using a constrained newwave methodology". Applied Ocean Research Vol. 23(4), pp. 221 – 234
[9] Tromans, P. S., A. R. Anaturk, & P. Hagemeijer (1991). "A new model for the kinematics of large ocean waves". *In Proc.First Intern. Confer. on Offshore and Polar Engineering,* Vol. 3, pp. 1–64.
[10] Hasselman, K. & et al. (1973). "Measurements of windwave growth and swell decay during the Joint North Sea Wave Project (JONSWAP)". *Deutschen Hydrographischen Zeitschrift*, Reihe A8. Nr. 12.
[11] Mitsuyasu, H. (1975). "Observations of directional spectrum of ocean waves using a cloverleaf buoy." Journal of Phys. Oceanogr. Vol. 16, pp. 750–760.
[12] Wheeler, J. (1970). "Method for calculating forces produced by irregular waves". Proc. Offshore Tech. Conf., Houston, USA. Vol. 1, pp. 71–82.
[13] Chatziioannou, K., V. Katsardi, and E. Mistakidis (2015). "The increasing importance of accurate calculation of the nonlinear extreme wave kinematics in the design of offshore platforms". To appear in International Maritime Association of the Mediterranean, IMAM2015, September 2015, Pula, Croatia.
[14] DNV (2000). DNV classification notes, environmental conditions and environmental loads, no. 30.5. Technical report, DNV.
[15] API (1993). API RP 2A LRFD, Recommended Practice for Planning, Designing and Constructing Fixed Offshore Platforms, Load and Resistance Factor Design, First edition. Technical report, API, USA.
[16] API (2008) Specification 4F: Specification for Drilling and Well Servicing Structures, Third edition.